JOURNAL OF NANO- AND ELECTRONIC PHYSICS
Vol. **16** No 4, 04004(5pp) (2024)

ЖУРНАЛ НАНО- ТА ЕЛЕКТРОННОЇ ФІЗИКИ
Том **16** № 4, 04004(5cc) (2024)

OPEN ACCESS

REGULAR ARTICLE

Exploration of Composition-Microstructure Relations in Polymer Nanocomposites: Intelligent Honey

A.B. Pawar[1], P. William[2,*] ✉, M.V. Kulkarni[3], Sharmila[4], D.K. Roy[5], N. Yogeesh[6]

[1] *Department of Computer Engineering, Sanjivani College Engineering, Kopargaon, SPPU, Pune, India*
[2] *Department of Information Technology, Sanjivani College Engineering, Kopargaon, SPPU, Pune, India*
[3] *Engineering Science and Humanities, Sanjivani College of Engineering, Kopargaon, SPPU, Pune, India*
[4] *Department of ECE, Raj Kumar Goel Institute of Technology, Ghaziabad, India*
[5] *Hyderabad Institute of Technology and Management, Gowdavelli Village, Medchal, Hyderabad*
[6] *Department of Mathematics, Government First Grade College, Tumkur, Karnataka, India*

(Received 10 April 2024; revised manuscript received 15 August 2024; published online 27 August 2024)

In polymer nanocomposites (PNCs), microstructure relationships encompass the intricate connections between nanofiller placement in the polymer matrix and resultant composite characteristics. The dispersion, size, shape and chemical interactions of nanofillers impact PNC performance, with thermo physical qualities varying based on composition. Establishing a universal composition-property relationship for PNCs is challenging due to their vast chemical diversity. This study proposes an innovative machine learning (ML) approach, the Intelligent Honey Bee-Fused Dynamic Random Forest (IHB-FDRF), to predict the composition-microstructure relationship of PNCs. Leveraging computational vision and image recognition, the IHB-FDRF predicts nanoparticles (NP) dispersion, validated through coarse-grained molecular dynamics simulations. The model forecasts NP arrangement in PNCs in latent space, translating to the radial distribution function (RDF) using the IHB-FDRF algorithm. The Mean Squared Error (MSE) in predictions, quantifying the average squared difference between predicted and actual values, is impressively low at 0.005 during the training phase, affirming the model's accuracy. The study's robustness is further confirmed by the overlap of latent values in both areas, signifying convergence between hidden characteristics and ensuring reliability across diverse contexts. In summary, this study gives significant findings on PNC microstructure relationships.

Keywords: Polymer nanocomposites (PNCs), Nanoparticle (NP), Radial distribution function (RDF), Intelligent Honey Bee-Fused Dynamic Random Forest (IHB-FDRF), Mean squared error (MSE).

DOI: 10.21272/jnep.16(4).04004 PACS number: 81.05.Qk

1. INTRODUCTION

Polymer nanocomposites (PNCs) are composed of several parts, with the framework as a polymer and the dispersion component having a minimum dimension of less than 100 nm. A Single nanoparticle should be uniformly disseminated in the matrix polymers for the perfect nanocomposite. The scattering condition of nanoparticles (NPs) is a major barrier to realizing the full scope of property improvement [1]. Polymers are strengthened with fillers of varying sizes to overcome limits and expand their uses. Nanoscale fillers have revolutionized polymer composites by improving their mechanical and chemical properties. Nanoscale fillers exhibit a distinctive length dimension of nanometers and range from isotropic to strongly anisotropic sheet-like or needle-like morphology [2]. Nanocomposites, made with nanoscale additives like fullerene, carbon nanotubes montmorillonite, graphene and mineral oxide, are gaining attention among researchers due to their unique characteristics. The 2D nanosheet filling outperforms 0D and 1D nanofillers owing to its much larger particular area [3]. PNCs have unique features when compared to basic matrix polymers and nanofillers, such as strong conductivity of electricity [4]. The microscopic configuration and dispersal of the nanofillers in polyamide media have a major impact on the final characteristics of the nanocomposite. Rheometry is a valuable tool for studying the microstructure of nanocomposite materials due to the relationship between the structure of networks and rheological characteristics [5]. Polymers are used to modify the microstructure of ceramics, resulting in nanocomposites. The microstructure of these nanocomposites is studied using scanning electronic microscope (SEM) and transmitted electronic microscope (TEM) methods. This process involves biological onium and change of procedures [6]. The microstructure of polymer composites, particularly the proportion of volumetric free fractions (f_r) and interfacial contact (β) among graphene and the matrix of polymers, plays a crucial role in determining their characteristics. β, which defines the substances dispersal declaration impacts stress dispersal and acoustical diffraction. Furthermore, the f_r influences transportation efficiency likes electric conductivity, stability in heat and gas/liquid resistance qualities. Despite significant

* Correspondence e-mail: william160891@gmail.com

Cite this article as: A.B. Pawar et al., *J. Nano- Electron. Phys.* 16 No 4, 04004 (2024) https://doi.org/10.21272/jnep.16(4).04004

strides achieved in the creation of polymer composites using beneficial electronic, mechanical and temperatures, there are few findings regarding microstructure (f_r and β) and the relation in these factors and features for PNCs [7]. PNCs' multiphase creation allows for the consideration of various measure connections, such as the matrix of micro-structural characteristics phase (s) anatomy, feasible crystal growth, cellular directions, the formation of cellular structures in foaming agents along with the application of NPs with various ratios of aspect and shapes, among additional variables [8].

The rest of this paper is structured as follows. The related works of polymer nanocomposites microstructure is examined in section 2 and section 3 discusses materials coupled with processes. In section 4, describe the results and the discussion session. Finally, in section 5, provide a conclusion and recommended future study directions.

2. RELATED WORKS

The study [9] used a complete phase-field framework to evaluate the disintegration reactions of PNCs with magnetic stimulation. The microstructure in the nanocomposite has been discovered to have a considerable impact on its breaking capacity and route. The study [10] addressed conceptual advances in polymer nanocomposites, which were mixed substances created by combining inorganic particles with natural polymers. That focused on several areas: synthesizing, phase conduct, processing, extrinsic areas and technical features. The study [11] summarized heat transfer mechanisms in polymer compound, including morphology, network organization and inter-chain connection. It highlighted current attempts to improve the thermal conductivity of nanostructured material polymers and nanocomposites. The research [12] determined nanofiller distribution in polymer salt solution that leads to improved fundamental, microstructural and electromechanical characteristics. The study [13] examined insulative polymers with conductive fillers (IPCFCPNCs) and conductive-fillers-based polymer nanocomposites (CFPNCs). These materials were utilized for strain meters for pressure, gas temperature and other sensor uses. The research [14] evaluated the impact of manganese dioxide nanowires (MnO2NWs) used as supplementary nanofiller on the network framework of carbon nanotubes (CNTs) and PNCs in a Carbon nanotube (CNT)/PNCs substrate. Adding MnO2NWs into PVDF/CNT specimens improved the dispersal of CNTs/PNCs, as shown through light and reflection of electron microscopes. The research [15] showed the pressured rotation was effective in producing antibiotic PNC fiber grids with graphene oxide (GO) nanosheets. Fiber grids have been reviewed using SEM, Raman spectroscopy, Raman visualization and Fourier-Transform infrared spectrum (FT-IR) to assess their morphology and chemical structure. The study [16] concentrated on the microstructure properties of shape memory polymer composites (SMPCs) packed with various carbon and silicate-based Nano/microparticles coupled with hybrid NPs. Silicates filler in SMPCs were classified based on their natural forms (1, 2 and 0 D) and the data required for customizing a suitable SMPC was discussed.

3. MATERIALS AND METHOD

This section investigates the complex interactions between composition and microstructure in polymer nanocomposites using an innovative method known as the Intelligent Honey Bee-Fused Dynamic Random Forest. The technique uses machine learning's computing capacity and unique insights inspired by honey bee activity to forecast how composition affects the microstructure of these sophisticated materials.

3.1 Framework

This study uses a phenomenological coarse-grained (CG) framework to analyze PNC. Kremer and Grest's coarse-grained bead-spring concept is used to depict chain polymers whereby a set of monomers interacts through their shape's Lennard-Jones (LJ) prospective in Eq. (1). The measurement of combination energy exchange is ϵ, while a monomer's diameter (d) is σ. Additionally, the Finitely Extensible Non-linear Elasticity (FENE) connects neighboring coarse-grained molecules in a polymer chains capability of the shape Eq. (2).

$$U(q) = 4\varepsilon\left[(\frac{\sigma}{q})^{12} - (\frac{\sigma}{q})^{6}\right] \tag{1}$$

$$F = -\frac{1}{2}LQ_0^2 \ln\left[1 - (\frac{q}{Q_0})^2\right] \tag{2}$$

Wherein $L = \frac{30 \in}{\sigma^2} Q_0 = 1.5\sigma$ with lengths of bonds $q \le Q_0$ and $F = \infty \quad q > Q_0$ at a threshold range of $q_d = 2.5\sigma$, the LJ connection among each monomer is shortened and reduced to zero. The NP (C) has been represented using the LJ capacity. The dimension of a NP ranges from 2σ to 5σ.To depict its appeal among NPs, the relationship among them is reduced and moved to zero over an elevation of $q_d = 2.5C$. The NP – NP interaction $\in_{(NP-NP)}$ differ from $0.2\in$ to $3.0\in$. The polymer – NP $\in_{(NP-NP)}$ communication varies between $0.5\in$ to $2.0\in$. At an acceptable distance, the relationship between the polymers and NP is shortened as well as reduced to zero $q_d = 2.5 \times \frac{C+c}{2}$. The link lengths in the copolymer vary from $N = 3.0$ to 52.

3.2 MD Modeling Data

This study simulates the PNC model using coarse-grained molecular dynamics (CGMD) considering various factors such as polymer – NP connection, NP quantity, NP – NP connection and NP – polymer length proportion. The resulting databases are utilized to teach and refine an ML system. The CGMD computations are run in an ideal collection with temperatures and pressures regulated by canonical thermostat and pressure regulators. To solve an equation of movement, that employs the Verlet-

Velocity technique with a time increment in 0.005τ. In $\tau = \sigma\sqrt{\frac{n}{\in}}$, operational simulations of MD, gather 8000 variations to compute the RDF for the framework. The run 100 MD models for different combinations of $\frac{S * Sl_A}{\in} = 1$ and $O^* = \frac{O\sigma^3}{\in} = 1$.The level of $NPs(\rho)$ is computed as a proportion that the amount of NPs to the optimum simulation package size. Diverse RDF properties, such as nanoscale phase division, steric stability and via bridge of the NP polymeric layer are obtained by combining these five variables. This study computes RDF in an 10σ interval. This study uses a box with a size of a fraction for RDF calculations. Thus, an RDF is a narrow-minded matrix of dimension one hundred. This study utilizes spatial coordinates for displaying an RDF for every set of composing variables. This analysis includes RDFs that vary from zero to three hundred in size. To depict an additional restricted spectrum of fluctuation, this research uses an exponential scale for the plot ordinates. To ensure consistency, graphic dimensions are set between zero and ten for abscesses as well as 0.05 and 350 for ordinates. The resulting RDF graph is shown as a gray-scale graphic, having a white line and black backdrop. This process generates 80 gray-scale images, with matching to a distinct group of 5 arrangement criteria.

3.3 Intelligent Honey Bee-Fused Dynamic Random Forest (IHB-FDRF)

The IHB-FDRF technique is used for studying composition-microstructure relationships in nanocomposites of polymers. This technique combines the flexibility of FDRF approach with clever elements influenced by IHBO cooperation. The research utilized IHBO, a nature-inspired optimization approach, to predict and analyze NP dispersion in polymer nanocomposites. Its adaptive and autonomous properties allowed for accurate predictions and a comprehensive understanding of the microstructure of PNCs. The FDRF constantly evolves through duration and reacts to shifts in data, resulting in a great tool for representing the intricate interactions as seen in polymeric nanocomposites supplies. The encoder compresses and represents input data in a lower-dimensional space, capturing essential features for prediction or classification tasks, particularly in IHB-FDRF, preparing and transforming data for machine learning analysis.

3.3.1 Intelligent Honey Bee Optimization (IHBO)

The IHBO method generates a sample at random of length M, where M is the overall amount of *NPs*. Nano fillers (Eq. (3)) is D-dimensional matrices representing single hired *NPs*. The $E(W_j)$ represents both the fitness level of the mixture and the volume W_j is the honey in an *NP*. Repetition durations for every source are restricted to "reduce", while the greatest number of iterations for the total populace is limited to maximum pages. The procedures are as follows.

$$W_j(j = 1,.....,M) \quad (3)$$

$$W_j^i = W_{\min}^i + rand(0,1)(W_{\max}^i - W_{\min}^i) \quad (4)$$

At random generate an acceptable response to *M*, when $j = 1$ up to *M*, */*j* denotes the D-dimensional vector element */. the recruited bee searches finding a suitable *NP* and evaluates its polymer rating to determine whether it is superior compared to its predecessor. When $j = 1$ up to *M*. $/*E(U_j) =$ novel source *NPs*, if U_j replaces W_j, if not then it is unchanged */.

$$U_j^i = W_j^i + \varphi_j^i(W_j^i - W_l^i) \quad (5)$$

$$E(W_j) < E(U_j) \quad (6)$$

The φ_j^i suggested approach generates a random value within [–1, 1] using the $\varphi \geq 0$ variables. The outcome falls within [0, 1].

3.3.2 Fused Dynamic Random Forest (FDRF)

The FDRF technique utilizes a decision tree structure for training and prediction. The algorithm employs bootstrapping and collections referred as baggage, to average forecasts across multiple decision trees and produce the end product. This research investigates the effectiveness of FDRF with various amounts of trees to discover the optimal quantity of reducing incorrect projections. This study created the RF regression structure via Tensor Flow. Fig. 1 shows how the regressor and decoder collaborate to predict the RDF of NPs in the matrix of the polymer.

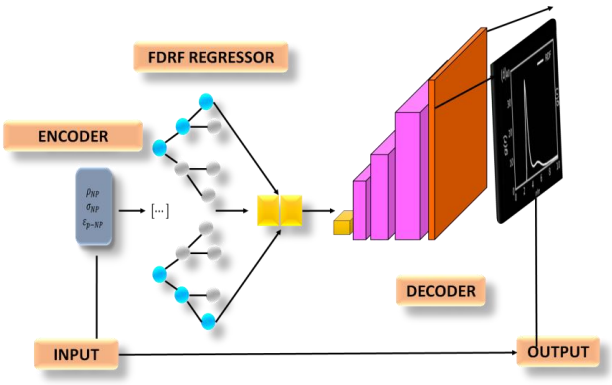

Fig. 1 – Linkage between the FDRFs Regressor and decoder

Construct the margin function as follows: assuming a group of classifications Eq. (7) and the training data taken at random from the shape for random vectors Z,W.

$$g_1(w), g_2(w),....., g_L(w) \quad (7)$$

$$mg(W,Z) = bu_l J(g_l(W) = Z) - \max_{i \neq Z} bu_l J(g_l(W) = i) \quad (8)$$

The J(.) represents an indication of function and the variance indicates how many votes the correct class receives at Wand *Z* when compared to the median score for every other category as well as the greater variance is more confident in the classification. The extrapolation mistake is represented by:

$$PE^{*} = O_{w,z}(mg(W,Z) < 0) \quad (9)$$

Subscripts like W and Z denote that the chance is across the W,and Z space. In random forests, equals with a high amount of forests, the powerful Principle of high Quantities and tree structure indicates that's the amount of trees grows, sequences like Θ_1.....PE^{*} is certainly convergence.

$$g_l(W) = g(W,\Theta_l) \quad (10)$$

$$O_{W,Z}(O_{\Theta}(g(W,\Theta) = Z) - \max_{i \neq Z} O_{\Theta}(g(W,\Theta) = i) < 0 \quad (11)$$

4. RESULT AND DISCUSSION

In this section, this research concentrates on IHB-FDRF training using RDF data. RDFs are transformed into 68×68 grayscale images for machine learning, as described in the technique section. To develop a self-coding method, this study produces a pair of data collections: training and validation. The validation along with training collections represents 90% and 30% of the entire RDF statistics, respectively. The IHB-FDRF is trained using 412 intervals. Fig. 2 shows that in the initial phases of training, the mean square error (MSE) decreases for the validation and training groups. The encoders reduce 68×68 images to a limited matrix with size eight. More about these analyses can be found in additional data. After training, assess the encoder's efficiency.

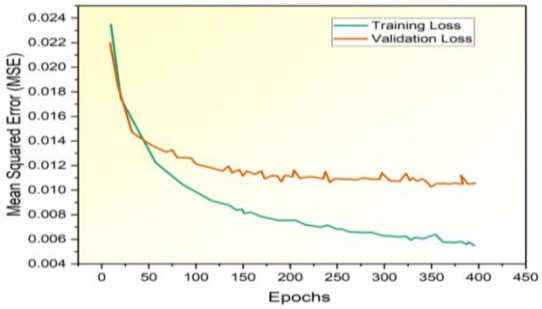

Fig. 2 – Training and validation loss of MSE

This study create an IHB-FDRF framework for predicting the latent area vector of RDF using the structure of a PNC. Each characteristic and goal has a value independently, ranging from 0 to 1. The standardized sample is randomly split into a pair of groups: first for training the IHB-FDRF regressor and another to test its efficacy. The training and test groups make up about 90% and 30% of the overall facts, respectively. This study adjusts the amount of tree structures in the IHB-FDRF to get the optimal design. Fig. 3 displays the MSE as an expression of tree structures in IHB-FDRF. The IHB-FDRF regressor performs optimally with over 26 decision trees.

The examination of the latent values acquired through projection reveals an interesting finding. The predicted and actual space latent levels exhibit a surprising degree of consistency. This relationship indicates a strong and reliable depiction of the fundamental features in the projection and actual spaces. This arrangement merely confirms the estimation process,

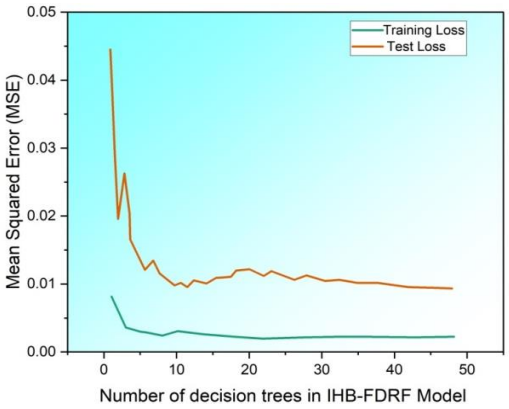

Fig. 3 – MSE as an expression of tree structures of IHB-FDRF

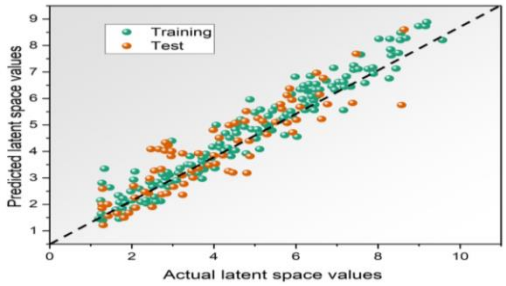

Fig. 4 – Training and testing value in latent space

but it improves the understanding and usability of the data obtained via these hidden variables. Fig. 4 shows the latent space values of training and testing groups.

5. CONCLUSION

This work delves into microstructure interactions in polymer nanocomposites (PNCs), highlighting the complex impact of nanofiller distribution within the polymer substrate on composite properties. The IHB-FDRF uses computational vision and image recognition to forecast nanoparticle (NP) dispersion, which is confirmed by coarse-grained molecular dynamics simulations. The model's capacity to anticipate NP arrangement in PNCs inside latent space and transform this information to the RDF using the IHB-FDRF method displays its flexibility. The prediction model's low MSE of 0.005 during the training phase demonstrates its accuracy, emphasizing its efficacy in capturing the intricate interactions among polymer nanocomposites. The study's robustness is further shown by the overlap of latent values, which indicates convergence across hidden properties and ensures the model's dependability across varied situations. Furthermore, the values of R2 (0.86%) and (0.99%)for the IHB-FDRF test and training sets, respectively, highlight the model dependability coupled with the promise for furthering our knowledge of PNCs. The overall research, this work not only provides useful insights into the microstructure interactions of PNCs, but it also proposes an effective ML technique which demonstrates improvements in material research and model prediction. The research will expand its scope by utilizing different nanofillers and evaluating the IHB-FDRF model's flexibility. It will also conduct dynamic simulations of nanoparticle interactions in PNCs, ensuring its robustness and generalizability through rigorous validation methodologies.

REFERENCES

1. A.D. De Oliveira, C.A.G. Beatrice, *Nanocomposites-Recent Evolutions* (Intech Open: London, UK: 2018).
2. S. Fu, Z. Sun, P. Huang, Y. Li, N. Hu, *Nano Mater. Sci.* **1** No 1, 2 (2019).
3. X. Sun, C. Huang, L. Wang, L. Liang, Y. Cheng, W. Fei, Y. Li, *Adv. Mater.* **33** No 6, 2001105 (2021).
4. J. Zhao, L. Wu, C. Zhan, Q. Shao, Z. Guo, L. Zhang, *Polymer* **133**, 272 (2017).
5. M. Kamkar, R. Salehiyan, T.B. Goudoulas, M. Abbasi, C. Saengow, E. Erfanian, S. Sadeghi, G. Natale, S.A. Rogers, A.J. Giacomin, U. Sundararaj, *Prog. Polym. Sci.* **132**, 101580 (2022).
6. W.R. Azzam, *Alexandria Eng. J.* **53** No 1, 143 (2014).
7. X. Han, T. Chen, Y. Zhao, J. Gao, Y. Sang, H. Xiong, Z. Chen, *Nanomaterials* **11** No 11, 2990 (2021).
8. H. Abbasi, M. Antunes, J.I. Velasco, *Prog. Mater. Sci.* **103**, 319 (2019).
9. Z.H. Shen, J.J. Wang, Y. Lin, C.W. Nan, L.Q. Chen, Y. Shen, *Adv. Mater.* **30** No 2, 1704380 (2018).
10. S.K. Kumar, V. Ganesan, R.A. Riggleman, *J. Chem. Phys.* **147** No 2, 020901 (2017).
11. C. Huang, X. Qian, R. Yang, *Mater. Sci. Eng.: R: Rep.* **132**, 1 (2018).
12. A. Arya, A.L. Sharma, *J. Phys. D: Appl. Phys.* **51** No 4, 045504 (2018).
13. S. Sharma, A. Verma, S.M. Rangappa, S. Siengchin, S. Ogata, *J. Mater. Res. Technol.* **26**, 5921 (2023).
14. M. Kamkar, E. Aliabadian, A. Shayesteh Zeraati, U. Sundararaj, *Phys. Fluid.* **30** No 2, 023102 (2018).
15. R.K. Matharu, T.A. Tabish, T. Trakoolwilaiwan, J. Mansfield, J. Moger, T. Wu, C. Lourenço, B. Chen, L. Ciric, I.P. Parkin, M. Edirisinghe, *J. Colloid Interface Sci.* **571**, 239 (2020).
16. M. Panahi-Sarmad, M. Abrisham, M. Noroozi, A. Amirkiai, P. Dehghan, V. Goodarzi, B. Zahiri, *Eur. Polym. J.* **117**, 280 (2019).
17. E.Champa-Bujaico, A.M. Díez-Pascual, A.L. Redondo, P. Garcia-Diaz, *Compos. Part B: Eng.* **269**, 111099 (2024).

Дослідження зв'язків між фазовим складом та мікроструктурою в полімерних нанокомпозитах: інтелектуальний підхід

A.B. Pawar[1], P. William[2], M.V. Kulkarni[3], Sharmila[4], D.K. Roy[5], N. Yogeesh[6]

[1] *Department of Computer Engineering, Sanjivani College Engineering, Kopargaon, SPPU, Pune, India*
[2] *Department of Information Technology, Sanjivani College Engineering, Kopargaon, SPPU, Pune, India*
[3] *Engineering Science and Humanities, Sanjivani College of Engineering, Kopargaon, SPPU, Pune, India*
[4] *Department of ECE, Raj Kumar Goel Institute of Technology, Ghaziabad, India*
[5] *Hyderabad Institute of Technology and Management, Gowdavelli Village, Medchal, Hyderabad*
[6] *Department of Mathematics, Government First Grade College, Tumkur, Karnataka, India*

У полімерних нанокомпозитах (PNCs) взаємозв'язки між мікроструктурою охоплюють складні зв'язки між розміщенням нанонаповнювача в полімерній матриці та кінцевими характеристиками композиту. Дисперсія, розмір, форма та хімічні взаємодії нанонаповнювачів впливають на продуктивність PNCs, причому теплофізичні властивості змінюються залежно від складу. Встановлення універсального зв'язку між складом і властивостями PNCs є складним завданням через їхню величезну хімічну різноманітність. У цьому дослідженні пропонується інноваційний підхід машинного навчання (ML), інтелектуальний динамічний випадковий ліс, об'єднаний медоносними бджолами (IHB-FDRF), для прогнозування зв'язку складу та мікроструктури PNCs. Використовуючи обчислювальне бачення та розпізнавання зображень, IHB-FDRF прогнозує дисперсію наночастинок (NP), перевірену за допомогою симуляції грубої молекулярної динаміки. Модель прогнозує розміщення NP у PNCs у латентному просторі, перекладаючи на функцію радіального розподілу (RDF) за допомогою алгоритму IHB-FDRF. Середня квадратична помилка (MSE) у прогнозах, яка кількісно визначає середню квадратну різницю між прогнозованими та фактичними значеннями, є вражаюче низькою і становить 0,005 під час фази навчання, що підтверджує точність моделі. Надійність дослідження додатково підтверджується перекриттям прихованих значень в обох областях, що означає конвергенцію між прихованими характеристиками та забезпечення надійності в різних контекстах. Підсумовуючи, це дослідження дає значні висновки щодо взаємозв'язків мікроструктури PNCs.

Ключові слова: Полімерні нанокомпозити (PNC), наночастинки (NP), функція радіального розподілу (RDF), інтелектуальний динамічний випадковий ліс, злитий медоносними бджолами (IHB-FDRF), середньоквадратична помилка (MSE).